LEVEL DECAY AND ORIENTATIONAL KINETICS OF THE RHODAMINE B MONOMER AND DIMER

James B. CLARK, Arthur L. SMIRL, Eric W. VAN STRYLAND, H.J. MACKEY and B.R. RUSSELL
Departments of Physics and Chemistry, North Texas State University, Denton, Texas 76203, USA

Received 5 September 1980; in final form 7 December 1980

The population kinetics and the rotational diffusion of the rhodamine B monomer and dimer were measured by using picosecond pulses from a mode-locked Nd : YAG laser to induce and time resolve the concentration-dependent transient absorption saturation of various aqueous solutions of this organic dye.

The widespread use and application of dye lasers has caused considerable attention to be focused on the spectroscopic characterization of commonly used organic dyes. It is well known that these organic molecules tend to aggregate and form dimers in solution [1–5]. Previous experimental studies [1–5] have measured the absorption, excitation, fluorescence, and phosphorescence spectra of both the monomeric and dimeric forms of this common dye. The primary decay mechanism for the excited state dimer appears to be non-radiative in nature. To our knowledge, there has been no measurement of this rapid, non-radiative excited-state dimer decay. Here, we report the use of picosecond absorption saturation techniques to time resolve and separate the rotational and excited- state kinetics of the rhodamine B monomer and dimer in aqueous solution. We observed a concentration-dependent subnanosecond decay that we attribute to a rapid non-radiative excited-state dimer lifetime.

The laser source for all data presented here was a passively mode-locked Nd : YAG system operating at 1.06 μm. A single pulse was extracted from the mode-locked train and amplified to produce a single pulse of measured gaussian spatial profile and gaussian temporal distribution. This single, gaussian pulse at 1.06 μm was then frequency doubled to produce a 25 ps optical pulse at 0.53 μm. Optical filters were inserted to remove any residual 1.06 μm radiation. For both experiments (fig. 1) the picosecond pulse at 0.53 μm was divided into two parts (pump and probe) and one part delayed with respect to the other by a con-

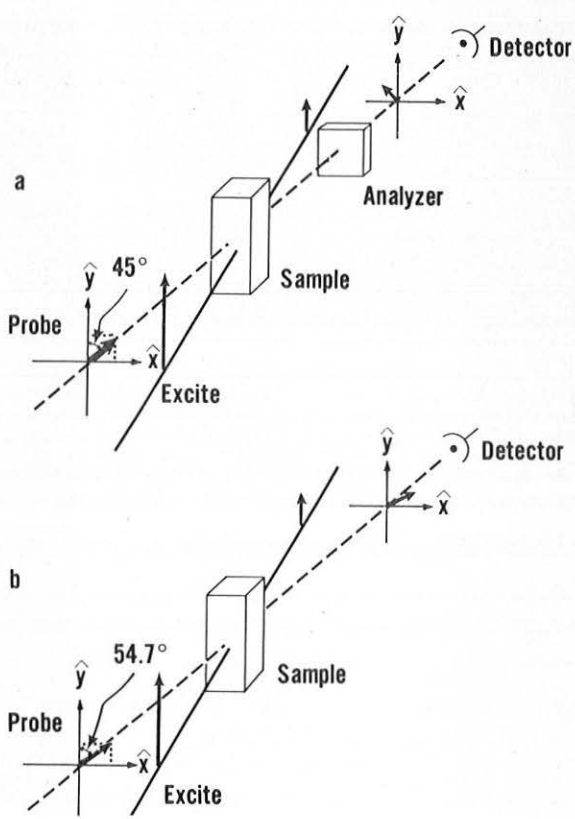

Fig. 1. Experimental configuration for the measurement of (a) the anisotropic absorption saturation and (b) the excited-state lifetime of aqueous solutions of rhodamine B.

trolled amount. The probe pulse was adjusted in all cases to be ≈5% of the pump pulse. Note that a wavelength of 0.53 μm lies near the isosbestic point in the absorbance spectra of the rhodamine B dye. The samples studied were various concentrations of rhodamine B in H_2O. Laser grade rhodamine B was obtained from Eastman Kodak and was used without further purification. H_2O was distilled prior to use. All studies were conducted at room temperature.

In the first experiment, the probe pulse polarization was rotated 45° with respect to the pump pulse as shown in fig. 1a. Both the pump and probe were focused onto the same 1 mm (fwhm) spot in a cell containing various concentrations of rhodamine B in aqueous solution. The intensity of the pump pulse (6 MW/cm^2) was sufficient to slightly saturate the absorption of those molecules partially aligned parallel to the pump. The pump and the probe were then separated spatially after they traversed the sample, and the transmission of the probe was measured through crossed polarizers, as shown. This experimental technique is identical to that used by Shank and Ippen [6] to measure the single component decay of DODCI.

Using the experimental configuration of fig. 1a, the probe transmission was measured as a function of time delay between pump and probe pulses for five concentrations of aqueous rhodamine B: 4.6×10^{-3}, 9.2×10^{-4}, 4.6×10^{-4}, 9.2×10^{-5}, and 4.6×10^{-5} M. The data for three concentrations are presented in fig. 2. The data for the 9.2×10^{-4} and 9.2×10^{-5} M solutions are omitted from fig. 2 for clarity.

Following anisotropic saturation of the sample by the pump pulse, the parallel polarization component of the probe experiences a larger transmission than the perpendicular component. The net result is a rotation of the probe polarization. The time-resolved measurement of the rotation of the polarization of the probe provides a convenient separation of the decay of the anisotropic saturation from the isotropic saturation. Assuming a two-component solution of dimers and monomers, modeled as simple three-level systems, the instantaneous transmission T_{cp} through the crossed polarizers of fig. 1a is given in the small saturation limit by

$$T_{cp}(t) = C[\eta(t) + (\sigma_d/\sigma_m)^2(D/M)\beta(t)]^2 , \qquad (1)$$

where C is a concentration-dependent constant, σ_d is

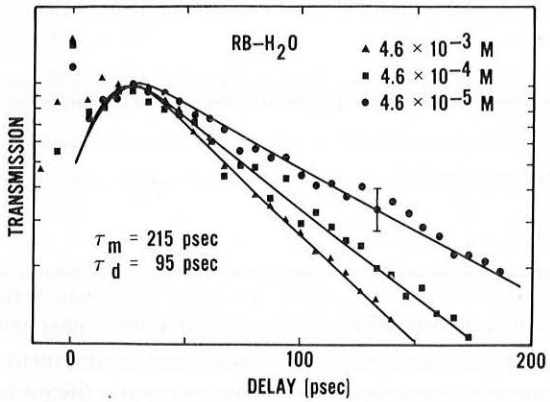

Fig. 2. The probe pulse transmission, in arbitrary units, as a function of time delay between pump and probe pulses for the geometry of fig. 1a and for three concentrations of rhodamine B in H_2O: 4.6×10^{-3}, 4.6×10^{-4}, and 4.6×10^{-5} M. The solid lines are numerical fits to the data, as discussed in the text. Two intermediate concentrations are not shown for clarity.

the dimer absorption cross section, σ_m the monomer absorption cross section, D the number of dimers, and M the number of monomers and where $\eta(t)$ and $\beta(t)$ are time-dependent integrals defined by

$$\eta(t) = \int_{-\infty}^{t} I_p(t') \exp[-(1/\tau_m)(t - t')]\, dt' \qquad (2)$$

and

$$\beta(t) = \int_{-\infty}^{t} I_p(t') \exp[-(1/\tau_d)(t - t')]\, dt' . \qquad (3)$$

In eqs. (2) and (3), $I_p(t)$ denotes the temporal pump intensity profile, and $1/\tau_m$ and $1/\tau_d$ are the overall monomer and dimer decay rates, respectively. Each overall decay rate is the sum of a level decay rate and a rotational diffusion rate:

$$1/\tau_m = 1/\tau_{lm} + 1/\tau_{om} \qquad (4)$$

and

$$1/\tau_d = 1/\tau_{ld} + 1/\tau_{od} , \qquad (5)$$

where τ_{lm} and τ_{om} are the monomer excited-state lifetime and orientational randomization time, respectively, and τ_{ld} and τ_{od} are the dimer excited-state lifetime and orientational randomization time. Clearly, the above equations have been written to include the finite width of the pump in determining the instantaneous analyzer transmission. If its pulsewidth

is negligible, $\eta(t)$ and $\beta(t)$ become simple exponentials. The effect of the finite width of the probe pulse on the transmitted probe energy, $S(\tau)$, is determined by convoluting the instantaneous analyzer transmission. $T_{cp}(t)$, with the probe temporal intensity profile, $I_s(t)$, to obtain

$$S(\tau) = \int_{-\infty}^{\infty} T_{cp}(t)\, I_s(t-\tau)\, \mathrm{d}t\,, \qquad (6)$$

where τ is the probe delay. Note that all effects of the coherent coupling between pump and probe near zero delay have been neglected in the above development. It is clear from the above equations (even if the probe and pump pulse widths are negligible) that the decay of the probe transmission (induced dichroism) is a complicated function of four parameters: the excited-state level decay of the monomer and the dimer and the orientational diffusion of the monomer and the dimer.

Extraction of measured decay constants by fitting experimental data to the above equations requires that the ratio of the number of dimers to number of monomers, D/M, for each concentration be determined and that the ratio of the dimer and monomer absorption cross sections, σ_d/σ_m, be known. Fortunately, the monomer–dimer equilibrium of aqueous rhodamine B can be described by the simple mass–action expression

$$K = 2x^2c/(1-x)\,, \qquad (7)$$

where K is the equilibrium constant, x is the mole fraction of monomer and c is the concentration. The mole fraction of monomer, x, and the dimer-to-monomer number ratio, D/M, were determined for concentrations between 4.6×10^{-3} and 4.6×10^{-5} M using an equilibrium constant [2] of 6.8×10^{-4} M/ℓ. These results are tabulated in table 1. In addition, a dimer-to-monomer cross section ratio, σ_d/σ_m, of 2.4 at 0.532 μm was extracted from the spectroscopic data of Selwyn and Steinfeld [2].

The solid lines in fig. 2 represent numerical fits of eqs. (1)–(6) to the experimental data using the constants supplied in table 1. The best visual fit to the data for all five concentrations (only three shown) was obtained for an overall monomer decay time τ_m = 215 ps and an overall dimer decay time τ_d = 95 ps. It is important to remember that these decay constants depend on both rotational diffusion and excited-state decay [see eqs. (4) and (5)]. The deviation of theory from experiment near zero delay is a result of neglecting coherent coupling effects.

Table 1
Equilibrium data for the concentration-dependent dimerization of aqueous rhodamine B

Concentration, c (M)	Mole fraction monomer, x	Dimer/monomer ratio: $D/M = (1-x)/2x$
4.6×10^{-3}	0.24	1.61
9.2×10^{-4}	0.45	0.61
4.6×10^{-4}	0.57	0.38
9.2×10^{-5}	0.82	0.11
4.6×10^{-5}	0.89	0.06

To facilitate the separation of the various rotational diffusion and excited-state decay times, a second separate set of concentration-dependent measurements was performed using a geometry in which the probe transmission was insensitive to rotational kinetics [7]. The experimental configuration, as shown in fig. 1b, was similar to that used in the first experiment, but differed in two important respects. The probe polarization was rotated to 54.7° with respect to the pump polarization and the analyzer polarizer was removed. Again the same five concentrations of aqueous rhodamine B were investigated using this technique to separately determine the monomer and dimer level decay. The data for three of the concentrations are shown in fig. 3.

The change in the instantaneous sample transmission (i.e., the difference between the transient transmission and the linear, Beer's law transmission) for the geometry of fig. 1b and for a two-component system *in the small saturation limit* is given by

$$\Delta T(t) = C'[\eta'(t) + (\sigma_d/\sigma_m)^2 (D/M)\beta'(t)]\,, \qquad (8)$$

where C' is a concentration-dependent constant and where $\eta'(t)$ and $\beta'(t)$ are time-dependent integrals given by

$$\eta'(t) = \int_{-\infty}^{t} I_p(t') \exp[-(1/\tau_{lm})(t-t')]\, \mathrm{d}t' \qquad (9)$$

and

$$\beta'(t) = \int_{-\infty}^{t} I_p(t') \exp[-(1/\tau_{ld})(t-t')]\, \mathrm{d}t'\,. \qquad (10)$$

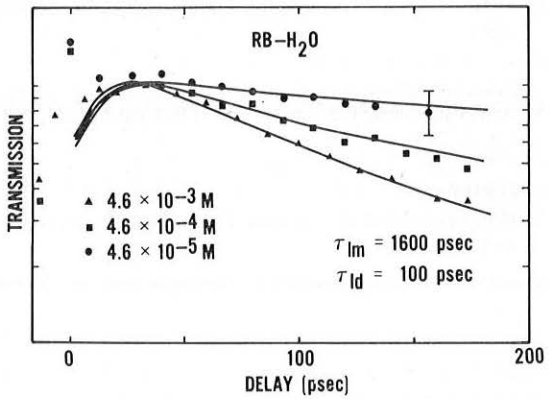

Fig. 3. The probe pulse transmission, in arbitrary units, as a function of time delay between pump and probe pulses for the geometry of fig. 1b and for three concentrations of rhodamine B in H_2O: 4.6 × 10^{-3}, 4.6 × 10^{-4}, and 4.6 × 10^{-5} M. The solid lines are numerical fits to the data, as discussed in the text. Two intermediate concentrations are not shown for clarity.

Notice that when the pump pulse width is negligible, $\eta'(t)$ and $\beta'(t)$ become simple exponentials that depend only on the level decay of the monomer and dimer, respectively, and $\Delta T(t)$ becomes a weighted, linear combination of these two simple exponentials. In the small saturation limit, then, this technique is insensitive to rotational effects. Again, the effect of the finite width of the probe pulse in determining the change in the transmitted probe energy, $\Delta S(t)$, is calculated by convoluting the instantaneous change in sample transmission, $\Delta T(t)$, with the probe temporal intensity profile, $I_s(t)$, to obtain

$$\Delta S(\tau) = \int_{-\infty}^{\infty} \Delta T(t)\, I_s(t-\tau)\, \mathrm{d}t\,. \qquad (11)$$

The lines in fig. 3 are numerical fits of eqs. (8)–(11) to the data. Excited-state decay constants of τ_{lm} = 1.6 ns and τ_{ld} = 100 ps were extracted for the monomer and dimer, respectively.

The level decay rate for the monomer was verified, in a third experiment, by time resolving the fluorescence decay of a 5 × 10^{-5} M solution following irradiation with a single 0.532 μm picosecond pulse using a fast detector–scope combination. The detector–scope system had a 600 ps (10–90% of signal) rise time and an identical 600 ps fall time. The fluorescence decay constant (e^{-1}), corrected for system response, for the 5 × 10^{-5} M solution (≈94% monomers) was 1.5 ns.

The overall decay constants τ_d and τ_m from the first experiment and the excited-state lifetimes τ_{lm} and τ_{ld} measured in the second were then used to determine the orientational randomization time for the monomer and dimer. Substituting τ_m = 215 ps and τ_{lm} = 1.6 ns into eq. (4), we obtain a diffusion time of τ_{om} = 250 ps for the monomer. Since the measured overall decay constant τ_d = 95 ps and the measured excited-state lifetime τ_{ld} = 100 ps are identical within experimental error, an accurate dimer rotational diffusion constant cannot be determined from eq. (5). It is easy to show, however, that the dimer orientational randomization time τ_{od} (and therefore the molecular volume) must be larger than that of the monomer.

Finally, we comment that all pump and probe experiments were performed at varying levels of saturation (15–50% of Beer's law) for each solution to ensure that we were operating in the small saturation limit consistent with eqs. (1)–(11). No measurable change in the decay rates was observed over this range of saturation levels.

Summarizing, we have used picosecond pump and probe techniques to measure the excited-state lifetimes of the rhodamine B monomer and dimer as 1.6 ns and 100 ps, respectively, and to determine the rotational randomization time of the monomer as 250 ps. The dimer rotational diffusion time was determined to be longer than that of the monomer. The extremely short excited-state dimer lifetime of 100 ps is an indication that the dimer may decay by a rapid non-radiative process. The exact nature of this process remains unknown and will require further study. In addition, the longer measured rotational decay time for the dimer provides physical evidence for the presence of a larger molecular species (dimer) in equilibrium with the monomer in the aqueous solution of rhodamine B. Finally, we emphasize that all of the above numerical lifetimes were extracted using a model that assumes that the orientational randomization times and excited-state lifetimes of both monomer and dimer are concentration independent, excluding energy transfer mechanisms between monomer and dimer. Experimental studies and calculations to determine the importance of such processes are underway.

This work was supported by The Robert A. Welch

Foundation, the North Texas State University Faculty Research Fund, and The Research Corporation.

References

[1] K.K. Rohatgi and G.S. Singhal, J. Phys. Chem. 70 (1966) 1695.
[2] J.E. Selwyn and J.I. Steinfeld, J. Chem. Phys. 76 (1972) 762.
[3] M.M. Wong and Z.A. Schelly, J. Phys. Chem. 78 (1974) 1891.
[4] T. Kajiwara, R.W. Chambers and D.R. Kearns, Chem. Phys. Letters 22 (1973) 37.
[5] R.W. Chambers, T. Kajiwara and D.R. Kearns, J. Phys. Chem. 78 (1974) 380.
[6] C.V. Shank and E.P. Ippen, Appl. Phys. Letters 26 (1975) 62.
[7] H.E. Lessing and A. von Jena, Chem. Phys. Letters 42 (1976) 213.